

# The Adsorption of Polyvinylpyrrolidone at the Mercury/Solution Interface

Tadashi YOSHIDA, Tetsuya OHSAKA, and Shoji TANAKA

Applied Electrochemical Laboratory, Graduate School of Science and Engineering, Waseda University, Nishi-Okubo, Shinjuku-ku, Tokyo

(Received March 13, 1971)

The adsorption of polyvinylpyrrolidone (PVP), known as a water-soluble polymer, at the electrolyte/DME interface was examined by observing the differential capacity *vs.* the time relation, under conditions where the adsorption process was mainly controlled by diffusion. In the case of a relatively low bulk concentration and a short adsorption time, the adsorption rate of PVP at  $-500$  mV(SCE) was controlled almost wholly by the diffusion of the adsorbate to the DME. The relation between the time required to attain the saturated adsorption and the bulk concentration was explained approximately by the Koryta equation, based on the linear diffusion. PVP showed no tendency to form multi-layers within the range of bulk concentrations and adsorption times observed. The maximum surface concentration of PVP decreased almost linearly with the increase in its mean molecular weight. The number of constitutive segments adsorbed per unit of area to form a monolayer at the interface was almost constant, independent of the mean molecular weight. The activation energy for the diffusion was found to be *ca.* 4.7 kcal/mol. On the basis of the results obtained, the configuration of PVP adsorbed at the interface was discussed.

Many water-soluble organic polymers are adsorbed strongly at the interface, and it takes some time to attain an adsorption equilibrium when the adsorption rate is mainly diffusion-controlled in a relatively dilute solution.<sup>1-3)</sup>

Polyvinylpyrrolidone (PVP),<sup>4)</sup> prepared first by Reppe, has characteristic properties of a good solubility, a strong adsorbability, protective colloid action, *etc.*<sup>5)</sup> Some papers<sup>6)</sup> on the properties of PVP in an aqueous solution have been published, and Jehring<sup>2)</sup> computed the maximum surface concentration ( $\Gamma_m$ ) of PVP dissolved in a potassium chloride solution by means of AC polarography. In the present paper, the adsorption of PVP will be investigated by observing the differential capacity in detail for the purposes of examining the diffusion behaviour of PVP in solution and discussing its configuration when adsorbed at the interface.

## Experimental

**Electrodes and Test Cell.** The dropping mercury electrode (DME) was used, and the flow rate ( $m$ ) and drop time ( $t_d$ ) of DME were as follows:  $m = 1.10\text{--}1.60 \times 10^{-4}$  g/sec,  $t_d = \text{ca. } 30$  sec/drop. The counter electrode was a cylindrical platinum net with a sufficiently large surface. The electrode potential was referred to the saturated calomel

electrode (SCE). The test cell and all parts of the mercury dropping equipment with a capillary, made of Pyrex glass except for the capillary, were connected tightly with ground glass joints without rubber stoppers, and the opening of capillary, prepared from a Molybdenum glass tube, was treated suitably with a tungsten carbide cutter.

**Materials.** Mercury was distilled twice *in vacuo* after having been treated in the usual way. Four kinds of chemical-grade PVP prepared by BASF were used without further purification; their mean molecular weights ( $\bar{M}$ ) were 10000, 26000, 37000, and 750000 respectively. All the solutions were prepared from guaranteed or purified reagents and triply-distilled water.

**Differential-capacity Measurements.** A precise impedance bridge of the transformer-connection type, equipped with a cathode-ray oscilloscope detector, was employed. The bridge was fed from the CR-type oscillator, where the sinusoidal wave of 1 kHz was adjusted by an attenuator so as to take an input voltage of *ca.* 10 mV<sub>p-p</sub>. A cylindrical platinum net, installed around a mercury drop, served as a counter electrode for the DC potentiostatic polarization of the test electrode and for the impedance measurements. On the assumption of a series-equivalent circuit of resistance and capacitance, the differential capacity at the mercury/solution interface was determined synchronously with a certain balance time from the beginning of drop growth. The measurements were conducted in an atmosphere of purified nitrogen.

## Theoretical

**Adsorption Behavior in the Diffusion-controlled Process.**

On the assumption of an adsorption process controlled simply by semi-infinite linear diffusion, the surface concentration ( $\Gamma_t$ ) of adsorbates on a mercury drop at a certain growth time,  $t$ , can be given by the well-known Koryta equation (1),<sup>7)</sup> derived from the Ilković formula:

$$\Gamma_t = 0.736 D^{1/2} a t^{1/2} \quad (1)$$

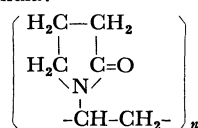
where  $\Gamma_t$  is expressed in mol/cm<sup>2</sup>, and  $t$ , in sec, and where  $D$  and  $a$  are the diffusion coefficient of adsorbates in cm<sup>2</sup>/sec and its bulk concentration in mol/cm<sup>3</sup>

1) H. Jehring, *J. Electroanal. Chem.*, **20**, 33 (1969); *ibid.*, **21**, 77 (1969); *Z. Phys. Chem.*, **229**, 39 (1965).

2) H. Jehring and E. Horn, *Monatsber. Deut. Akad. Wiss. Berlin*, **10**, 295 (1968).

3) P. W. Boad, D. Britz, and R. V. Holland, *Electrochim. Acta*, **13**, 1633 (1968).

4) Molecular formula:



5) R. L. Davidson and M. Sittig, eds., "Water-Soluble Resins," Reinhold Pub. Corp., New York (1962), p. 110.

6) B. Jirgensons, *Makromol. Chem.*, **6**, 30 (1951); W. Scholtan, *ibid.*, **7**, 209 (1951); J. Hengstenberg and E. Schuch, *ibid.*, **7**, 236 (1951); L. E. Miller and F. A. Hamm, *J. Phys. Chem.*, **57**, 110 (1953).

7) J. Koryta, *Collect. Czech. Chem. Commun.*, **18**, 206 (1953).

respectively. According to Frumkin,<sup>8)</sup> the relation between the differential capacity and the surface coverage ( $\theta$ ) is written as follows:

$$C = C_{\theta=1}\theta + C_{\theta=0}(1-\theta) \quad (2)$$

where  $C_{\theta=1}$  and  $C_{\theta=0}$  are the differential capacities per unit of area at  $\theta=1$  and  $\theta=0$  respectively. Assuming  $\theta = \Gamma_t/\Gamma_m$ , we obtain from Eqs. (1) and (2):

$$C = C_{\theta=0} - K a t^{1/2} \quad \text{for } t < t_m \quad (3)$$

where  $K = 0.736(C_{\theta=0} - C_{\theta=1})D^{1/2}\Gamma_m^{-1}$

$\Gamma_m$  and  $t_m$  are the maximum surface concentration of the adsorbates and the time required to attain the saturated adsorption respectively. Equation (3) holds only in the case of  $t < t_m$  where the adsorption is diffusion-controlled. On the other hand, in the case of  $t > t_m$ , where the adsorption equilibrium is always attainable and where  $\theta=1$ :

$$C = C_{\theta=1} \quad \text{for } t > t_m \quad (4)$$

It is shown by Eq. (3) that, if  $t$  is kept constant,  $C$  changes linearly with  $a$ , while if  $a$  is constant,  $C$  varies linearly with  $t^{1/2}$ .  $\Gamma_m$  can be computed from the experimental data by means of Eq. (3) if the value of  $D$  is given. At 25°C, the surface area  $A_t$  (cm<sup>2</sup>) of a mercury drop at its growth time,  $t$ , is given by the mercury flow rate,  $m$ , as:

$$A_t = 0.85m^{2/3}t^{2/3} \quad (5)$$

Therefore, the observed differential capacity,  $C_E$  ( $\mu\text{F}$ ), is written as follows from Eqs. (3), (4), and (5):

$$C_E = CA_t = 0.85C_{\theta=0}m^{2/3}t^{2/3} - 0.85Km^{2/3}at^{7/6} \quad (6)$$

for  $t < t_m$

$$C_E = C_{\theta=1}A_t = 0.85C_{\theta=1}m^{2/3}t^{2/3} \quad \text{for } t > t_m \quad (7)$$

*Application of Koutecký-type Equation.*<sup>9)</sup> The deviation from the Koryta equation can be explained by the Koutecký equation, in which  $\Gamma_t$  is given by Eq. (8), including the supplementary term based on the spherical diffusion:

$$\Gamma_t = 0.736D^{1/2}at^{1/2}(1 + 3.47D^{1/2}m^{-1/3}t^{1/6}) \quad (8)$$

The (9) and (4)' relations are obtained from Eq. (8) instead of from the (3) and (4) formulae:

$$\text{when } t < t_m, \quad C = C_{\theta=0} - K a t^{1/2}(1 + 3.47D^{1/2}m^{-1/3}t^{1/6}) \quad (9)$$

$$\text{if } t > t_m, \quad C = C_{\theta=1} \quad (4)'$$

## Results

*Differential-capacity vs. Potential Curves.* Figure 1 shows the differential capacity vs. potential curves in 1 N sulfuric acid solutions containing PVP ( $\bar{M}=10000$ ) of various concentrations under a fixed balance time,  $t_B$ . Relations similar to those in Fig. 1 can be obtained with various  $t_B$  values under a fixed value of  $a$  instead of  $t_B$ . In Fig. 1, the peak due to the ad- or desorption of PVP is found at a noble potential of ca. 75 mV(SCE), whereas no peak is given at the less noble side within the potential range observed, and the differential capacity decreases

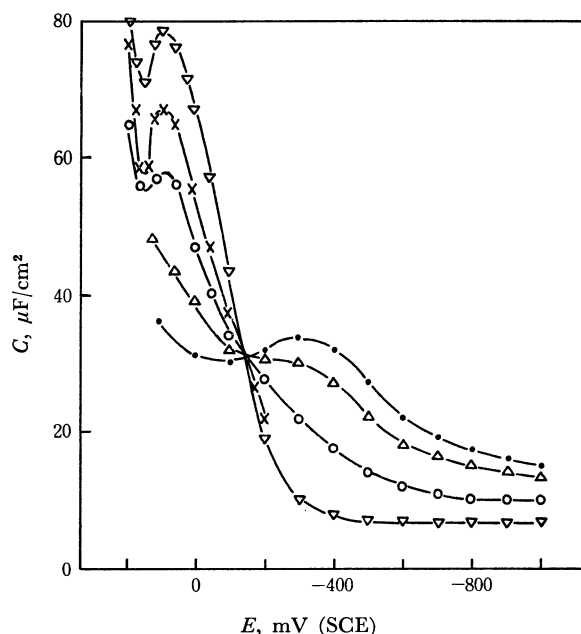


Fig. 1. Differential capacity vs. potential curves. 30.0°C,  $t_B$  (balance time)=15 sec, 1 N sulfuric acid+PVP ( $\bar{M}=10000$ ); (—○—: PVP 0 mg/l, —△—: 5 mg/l, —□—: 10 mg/l, —×—: 20 mg/l, —▽—: 50 mg/l)

on the less noble side, while it increases in the peak potential region with an increasing  $a$  (or  $t_B$  value). The dependence of the capacity on  $t_B$  may be understood in terms of the diffusion-controlled adsorption, where the adsorbed PVP increases with the time. Furthermore, it is found that the minimum differential capacity, ( $C_{min}$ ), due to the adsorption equilibrium or saturation is nearly constant independent of the value of  $a$  or  $t_B$  within the less noble potential range, while the peak potential is practically independent of the value of  $a$  or  $t_B$ .

Adsorption attains to its equilibrium or saturation at ca. -500 mV(SCE) near the zero-charge potential of mercury upon a reasonable increase in  $a$  (or  $t_B$ ), as may be seen in Fig. 1. Therefore, the interfacial behaviour of PVP will be discussed in most cases at -500 mV(SCE), where the saturated absorption is always attained.

*Observed Capacity vs. Time Curves.* Figure 2 shows examples of  $C_E$ - $t$  curves at -500 mV(SCE) in 1 N sulfuric acid solutions with various values of the concentration of PVP ( $\bar{M}=750000$ ).

In Fig. 2, the  $C_E$  for the saturated adsorption with PVP or for the blank solution may be seen to increase with  $t^{2/3}$  or  $A_t$  [cf. Eq. (5) or (7)]. In the diffusion-controlled process [cf. Eq. (6)],  $C_E$ - $t$  curves are depressed with  $a$ , and each curve has a tendency to coincide with the saturated adsorption curve. Diagrams analogous to Fig. 2 were always obtained with PVP's of various  $\bar{M}$  values, where for instance, the depression of  $C_E$  by the PVP of  $\bar{M}=10000$  was about three times that by the PVP of  $\bar{M}=750000$  under given  $a$  and  $t_B$  values.

*Oscillograms Observed with a PVP Solution.* The oscillograms obtained by the impedance bridge are

8) A. N. Frumkin, *Z. Phys.*, **35**, 792 (1926).

9) A. N. Frumkin and B. B. Damaskin, "Modern Aspects of Electrochemistry," No. 3, Butterworths, London (1964), p. 149.

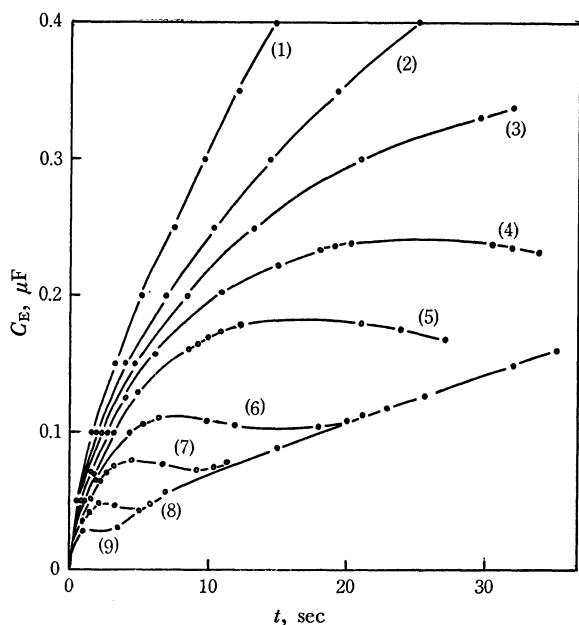


Fig. 2. Observed differential capacity *vs.* time curves.

Observed at  $-500$  mV (SCE),  $20.5^{\circ}\text{C}$ ,  $1$  N sulfuric acid  
(1)  $1$  N sulfuric acid + PVP ( $\bar{M}=750000$ ), (2) PVP  $15$  mg/l,  
(3)  $30$  mg/l, (4)  $40$  mg/l, (5)  $50$  mg/l, (6)  $75$  mg/l, (7)  
 $100$  mg/l, (8)  $150$  mg/l, (9)  $200$  mg/l

of a simple X type in the case of a blank solution, while they reveal distorted figures in the presence of PVP. Typical cases are shown in Photo. 1 and Fig. 3, where remarkable distortions of figures are revealed in the transient course from the diffusion-controlled process to the saturated adsorption. The oscillograms in Photo. 1 were obtained in a  $1$  N sodium sulfate solution containing  $25$  mg/l PVP. A figure corresponding to Photo. 1 is shown in Fig. 3, where the three values of the bridge capacitance adjusted

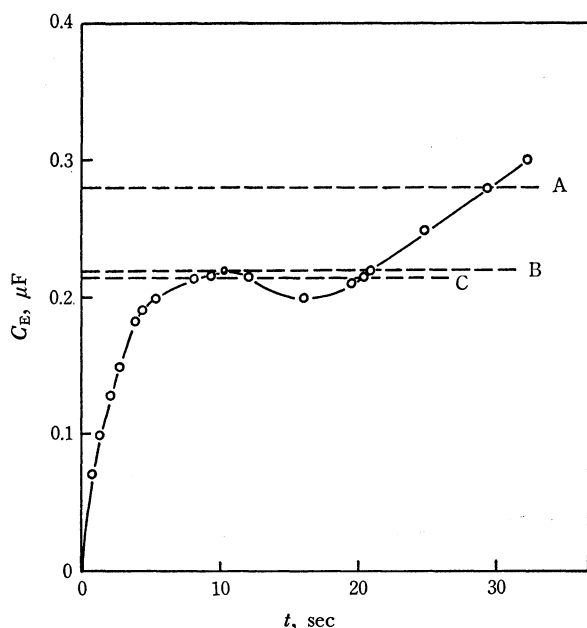


Fig. 3. Observed differential capacity *vs.* time curve connected with Photo. 1.

Observed at  $-500$  mV (SCE),  $20.5^{\circ}\text{C}$ ,  $1$  N sodium sulfate + PVP ( $\bar{M}=10000$ )  $25$  mg/l, adjusted capacitance; (A:  $0.280$   $\mu\text{F}$ , B:  $0.220$   $\mu\text{F}$ , C:  $0.215$   $\mu\text{F}$ )

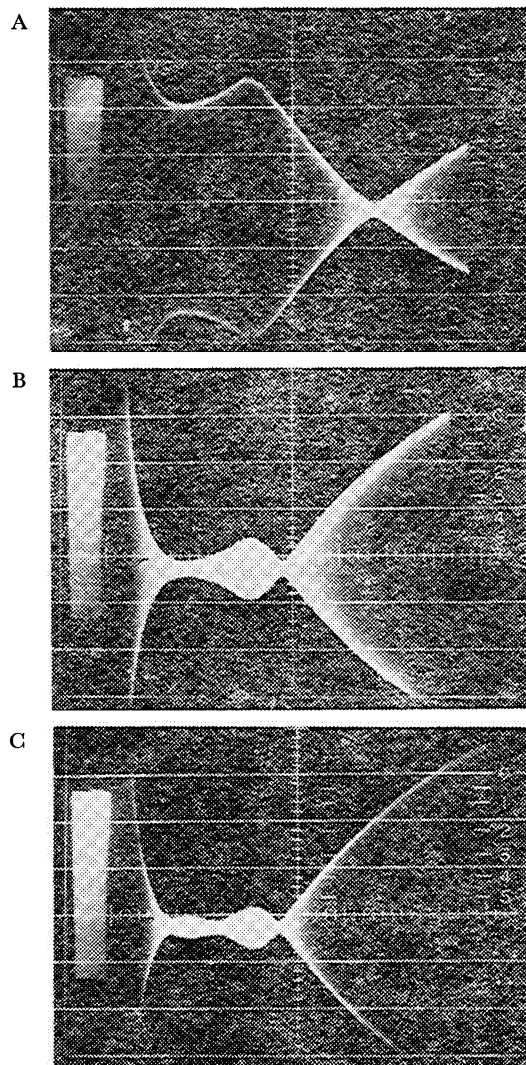


Photo. 1. Oscillograms for the bridge balance.

$1$  N sodium sulfate + PVP ( $\bar{M}=10000$ )  $25$  mg/l, X:  $5$  sec/div., Y:  $2$  V/div., "A", "B", and "C" correspond to each one in Fig. 3.

are given by dashed lines. Figure 3, showing  $1$  N sodium sulfate solution, is similar to Fig. 2, showing  $1$  N sulfuric acid solution. In the case of "C" in Photo. 1, three balance times ( $t_B$ ) are given, as to be expected from the three points of intersection in the order. It may be considered that the first two balance times are attributable to the diffusion-controlled processes, whereas the last one is due to the saturated adsorption. Similarly, the first and second  $t_B$  values for the "B" case in Photo. 1 or Fig. 3 may be due to the diffusion-controlled process and to the saturated adsorption respectively. Next, the balance time related to the "A" case in Photo. 1 or Fig. 3 may be due to the saturated adsorption, while the preceding distortion of the oscillogram is to be expected from the shape of the  $C_E$ - $t$  curve in Fig. 3. A figure similar to that in Photo. 1 can be obtained from such data as are shown in Fig. 3 on the assumption that the input admittance due to the unbalanced bridge is approximately proportional to the voltage found on the screen to the detector.

*Temperature Dependence of  $C$  *vs.*  $t$  Curves.*

Figure

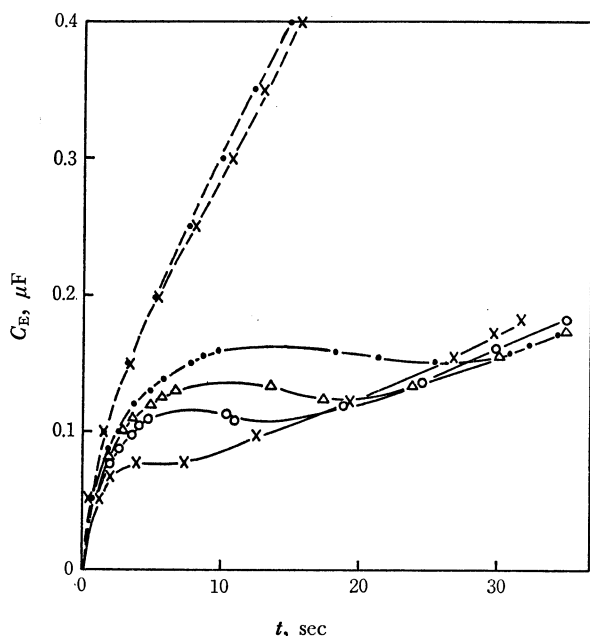


Fig. 4. Observed differential capacity *vs.* time curves obtained at various temperatures. Obtained at  $-500$  mV (SCE),  $20^\circ\text{C}$ ,  $1$  N sulfuric acid; (---:  $20^\circ\text{C}$ , --x--:  $60^\circ\text{C}$ ),  $1$  N sulfuric acid + PVP ( $\bar{M}=10000$ )  $20$  mg/l; (---:  $20^\circ\text{C}$ , -△-:  $30^\circ\text{C}$ , -○-:  $40^\circ\text{C}$ , -x-:  $60^\circ\text{C}$ )

4 shows the temperature dependence of the  $C_E$ - $t$  curves observed in a  $1$  N sulfuric acid solution containing PVP ( $\bar{M}=10000$ ) of  $20$  mg/l.

In Fig. 4, the difference between the two curves at  $20$  and  $60^\circ\text{C}$  is nearly negligible in the case of a blank solution. For the solution containing PVP, the time required to attain the saturated adsorption is about  $25$  sec at  $20^\circ\text{C}$ , and it decreases as the temperature rises. The saturated adsorption curves vary somewhat with the temperature, but the differences among them are so small that they are negligible within the temperature range from approximately  $20$  to  $60^\circ\text{C}$ .

### Discussion

#### Application of the Koryta Equation.

The variation in the differential capacity,  $C$ , with the drop-growth time,  $t$ , or with the bulk concentration,  $a$ , is expressed by Eq. (3) in the diffusion-controlled process, where  $t < t_m$ . As may be seen from Figs. 5 and 6 related to the PVP of  $\bar{M}=750000$ ,  $C$  decreases linearly with  $t^{1/2}$  or  $a$ , as to be expected from Eq. (3); it attains a constant value in each case at a certain values of  $t$  or  $a$ , as to be expected from Eq. (4). The constancy of  $C$  shows that the saturated adsorption is achieved. The more  $a$  or  $t_B$  increases, the steeper the slope of the curve becomes, as may be seen in Figs. 5 and 6. The curves in Figs. 5 and 6 always consist of two linear portions. It is possible to find the time  $t_m$  or the bulk concentration,  $a_m$ , necessary to attain  $\Gamma_m$  under a certain value of  $a$  or  $t_B$  from the intersection of these two lines.

It may be concluded that PVP is adsorbed to form the monolayer at the interface, since the minimum differential capacity ( $C_{\min}$ ) observed in the saturated

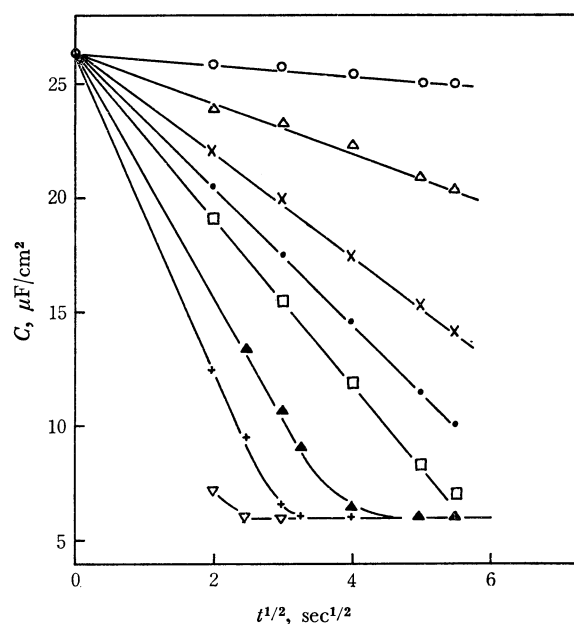


Fig. 5. Differential capacity *vs.* square root of time curves. Observed at  $-500$  mV (SCE),  $20.5^\circ\text{C}$ ,  $1$  N sulfuric acid + PVP ( $\bar{M}=750000$ ); (---:  $5$  mg/l, -△-:  $15$  mg/l, -x-:  $30$  mg/l, ---:  $40$  mg/l, -□-:  $50$  mg/l, -▲-:  $75$  mg/l, -+-:  $100$  mg/l, -▽-:  $150$  mg/l)

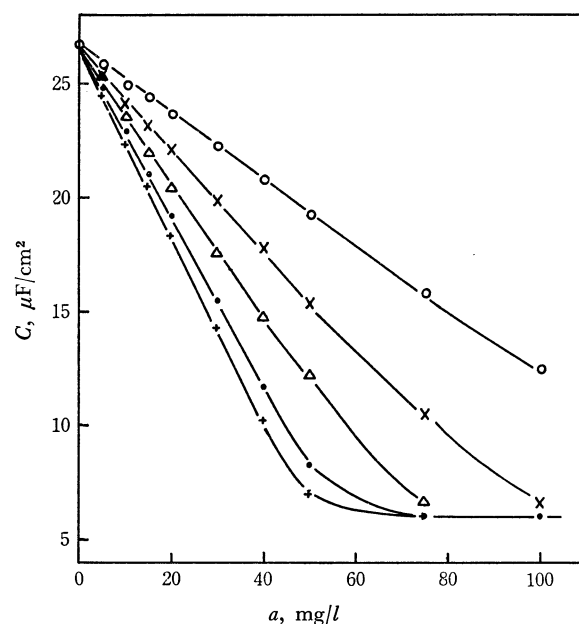


Fig. 6. Differential capacity *vs.* bulk concentration curves. Observed at  $-500$  mV (SCE),  $20.5^\circ\text{C}$ ,  $1$  N sulfuric acid + PVP ( $\bar{M}=750000$ ); (---:  $t_B=4$  sec, -x-:  $9$  sec, -△-:  $16$  sec, ---:  $25$  sec, -+-:  $30$  sec)

adsorption range is approximately constant independent of  $a$  or  $t$  (the drop growth or balance time), as may be seen in Fig. 5 or 6.

*Saturation Time related to Concentration.* The Koryta equation (1) may be modified as follows:

$$\left. \begin{aligned} \log t_m &= -2 \log a + K' \\ \log t &= -2 \log a_m + K' \end{aligned} \right\} \quad (10)$$

or:

$$\log t = -2 \log a_m + K'$$

where  $K' = 2 \log [\Gamma_m / (0.736D^{1/2})]$

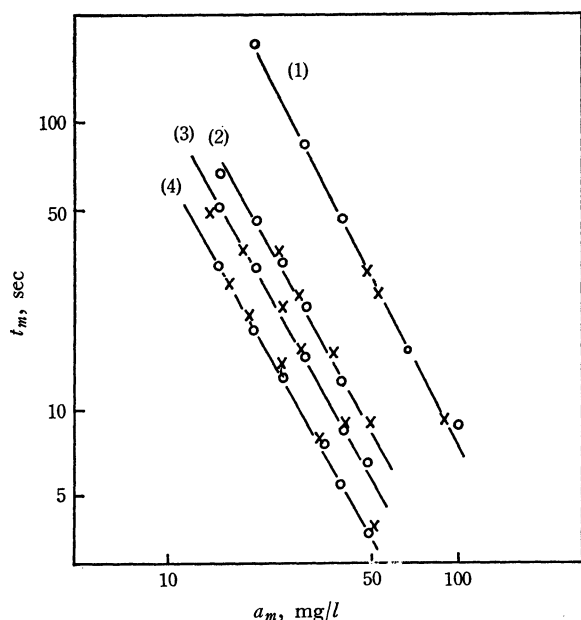


Fig. 7. Time required to attain the saturated adsorption vs. bulk concentration curves. Observed at  $-500$  mV (SCE),  $20.5^\circ\text{C}$ ,  $1\text{ N}$  sulfuric acid + PVP solutions,  $\circ$ —: derived from  $C$ - $t^{1/2}$  curves,  $\times$ —: derived from  $C$ - $a$  curves, (1): PVP:  $\bar{M}=750000$ , (2):  $37000$ , (3):  $26000$ , (4):  $10000$

In Fig. 7, typical plots of  $\log t_m$  vs.  $\log a$  and  $\log a_m$  vs.  $\log t$  are derived from Figs. 5 and 6 with four kinds of PVP. Each plot in Fig. 7 reveals an approximately straight line with a slope deviating by *ca.*  $-5\%$  from the expected value of  $-2$ . Moreover,  $t_m$  at a certain definite value of  $a$  becomes longer with an increase in the mean molecular weight, as may be seen from Fig. 7; this tendency may result from the lowering of the diffusion coefficient due to the increase in  $\bar{M}$ .

#### Reexamination of the Use of the Koryta Equation.

Typical  $C$ - $t^{1/2}$  and  $C$ - $a$  plots based on the Koryta equation are shown in Figs. 5 and 6 with the PVP of  $\bar{M}=750000$ , the  $K$  value in Eq. (3) can be calculated from the slope of each curve.  $\Gamma_m$  can be obtained from the value of  $K$  if the diffusion coefficient is known. However, the value of  $K$  obtained from the curves in Fig. 5 or 6 shows a slight dependence on  $a$  or  $t_B$ , *i.e.*, the values of  $K$  obtained from the curves in Fig. 5 slightly decrease with an increase in  $a$ , while the value derived from the curves in Fig. 6 slightly rises with  $t_B$ . Therefore,  $\Gamma_m$  is computed by means of the mean value of  $K$  based on the values of the diffusion coefficient<sup>10)</sup> as estimated by the Stokes-Einstein equation or experimentally obtained. The dependence of  $K$  on  $a$  or  $t_B$  may be attributable to the variation in the diffusion coefficient with the concentration, or to the effect of the supplementary term of the Koutecký type given in Eq. (9), which was deduced on the basis of

10) The values of the diffusion coefficient of PVP in the literature<sup>9)</sup> as estimated by the Stokes-Einstein equation and as observed with the hanging mercury electrode,<sup>11)</sup> are  $10.3 \times 10^{-7} \text{ cm}^2/\text{sec}$  for  $\bar{M}=10000$ ,  $7.3 \times 10^{-7}$  for  $\bar{M}=26000$ ,  $5.1 \times 10^{-7}$  for  $\bar{M}=37000$ , and  $1.2 \times 10^{-7}$  for  $\bar{M}=750000$ .

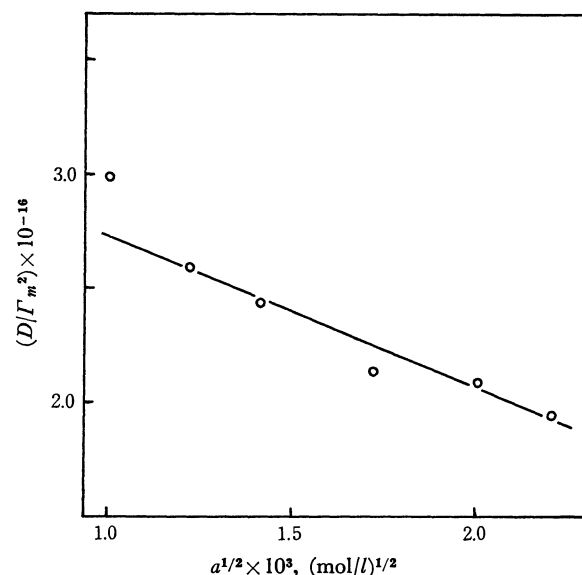


Fig. 8. Concentration dependence of diffusion coefficient for PVP. Observed at  $-500$  mV (SCE),  $20.5^\circ\text{C}$ ,  $1\text{ N}$  sulfuric acid + PVP ( $\bar{M}=10000$ ) solutions

the spherical diffusion under a constant  $\Gamma_m$  value, independent of  $a$ .

Friedman *et al.*<sup>12)</sup> found a linear relation between the diffusion coefficient and the square root of the bulk concentration for some organic substances (*e.g.*, dextrose, sucrose). An example of the  $(D/\Gamma_m^2)$  vs.  $a^{1/2}$  plot is shown in Fig. 8, where  $(D/\Gamma_m^2)$  has been calculated from the  $K$  derived from the slope of the  $(C$  vs.  $t^{1/2})$  relation at a given  $a$  of PVP ( $\bar{M}=10000$ ). As may be seen from Fig. 8,  $(D/\Gamma_m^2)$  shows an approximately linear dependence on the square root of the concentration of PVP. The linear relationship between  $(D/\Gamma_m^2)$  and  $a^{1/2}$  in Fig. 8 suggests that the dependence of  $K$  on  $a$  is attributable to the variation in the diffusion coefficient with  $a$  to a certain extent.

A slight deviation of the  $(D/\Gamma_m^2)$ - $a^{1/2}$  relation from linearity may be expected on the basis of the Koutecký equation, in which the effect of the spherical diffusion is taken into consideration. In Eq. (9), the slope of  $C$  vs.  $a$  relation shows  $-Kt^{1/2}(1+3.47D^{1/2}m^{-1/3}t^{1/6})$  instead of  $-Kt^{1/2}$  in the Koryta Equation (1). The value of  $K$  obtained on the basis of the Koryta Equation (1) should be modified to  $K(1+3.47D^{1/2}m^{-1/3}t^{1/6})$  in the case of the spherical diffusion, which may be expected to increase with the time. In fact, the value of  $K$  obtained from the  $C$ - $a$  curve by means of the Koryta equation increases slightly with  $t_B$  as has previously been stated.<sup>13)</sup>

In short, the variation in the  $K$  derived from the Koryta equation may be attributed to the concentration dependence of the diffusion coefficient or to the effect of the spherical diffusion. The deviation of

11) This Bulletin, to be published.

12) L. Friedman and P. G. Carpenter, *J. Amer. Chem. Soc.*, **61**, 1745 (1939).

13) In the case of  $\bar{M}=10000$ , for example, the  $K$  values derived from the Koryta equation were  $1.98 \times 10^9$ ,  $2.07 \times 10^9$ , and  $2.19 \times 10^9$  for  $t_B=4$ ,  $8$ , and  $16$  sec respectively.

the slope by *ca.*  $-5\%$  from the expected value of  $-2$  in Fig. 7 may be explained by the change in the diffusion coefficient or the effect of the spherical diffusion discussed above. It should be noted that the Koryta equation is approximately applicable to the present system within an error of  $10\%$ .

**Temperature Dependence of the Diffusion Coefficient.** The temperature dependence of the  $C_E$ - $t$  relation is shown in Fig. 4 for the case with a  $1\text{ N}$  sulfuric acid solution containing  $20\text{ mg/l}$  of PVP ( $\bar{M}=10000$ ), and a linear relation is obtained by plotting  $\log [D_T/D_{(273+20)}]$  to  $T$  or  $1/T$ ,<sup>14)</sup> where the value of  $(D_T/D_{(273+20)})$  is derived from the  $[(t_m \text{ at } T^\circ\text{K})/(t_m \text{ at } 273+20^\circ\text{K})]$  ratio with the Koryta equation at a given  $a$  on the assumption that  $\Gamma_m$  is constant independent of  $T$  under the present conditions. The temperature coefficient ( $\alpha$ ) of the diffusion coefficient and the activation energy ( $Q$ ) of the diffusion are found to be about  $0.025$  and  $4.7\text{ kcal/mol}$  respectively for the present case. The value of  $Q$  mentioned above may be reasonable for the diffusion process of PVP ( $\bar{M}=10000$ ).

**Configuration of PVP at the Interface.** By plotting  $\log \Gamma_m$  against  $\log \bar{M}$  for four kinds of PVP, we obtain an approximately linear relation with a slope of nearly  $-1$ , as shown in Fig. 9. From this linear relation,  $\bar{M}\Gamma_m = \text{const.}$  can be obtained; this means that  $\bar{P}/S$  is constant, where  $\bar{P}$  is the degree of polymerization or the number of segments, and  $S$ , the area of the electrode surface occupied by  $1\text{ mol}$  of the adsorbed molecule, that is,  $S = \Gamma_m^{-1}$ . Consequently, it follows that the adsorbed number of the constitutive segment related to PVP at the interface is constant, independent of  $\bar{M}$ , and that the value of  $\bar{P}$  per unit of area can be estimated from Fig. 9 to be *ca.*  $4.0 \times 10^{14}\text{ seg./cm}^2$ .

The geometrical form of the dissolved PVP molecule in the bulk of the solution was assumed to be a randomly-coiled polymer chain or a revolving ellipsoid.<sup>6)</sup> It seems, in the present case, that the geometrical form of PVP in the bulk of the solution may be close to a sphere consisting of a randomly-coiled chain, since the  $D$  of PVP, derived from the Stokes-

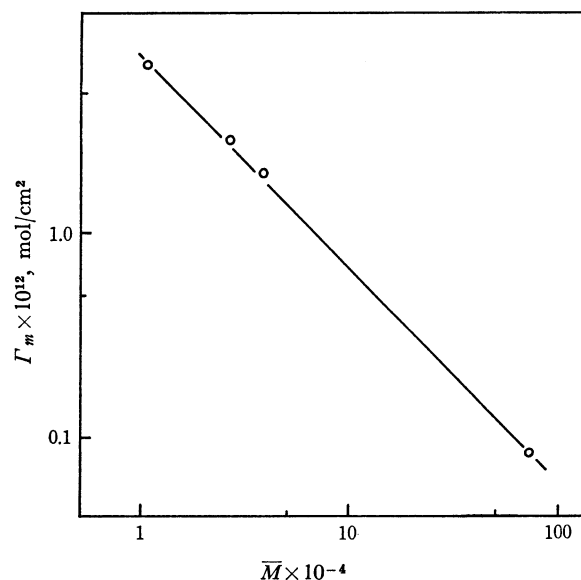


Fig. 9. Maximum surface concentration *vs.* mean molecular weight curve. Observed at  $-500\text{ mV (SCE)}$ ,  $20.5^\circ\text{C}$ ,  $1\text{ N}$  sulfuric acid + PVP solutions

Einstein relation assuming a spherical form, is approximately consistent with the value observed.<sup>11)</sup>

Nevertheless, the spherical form of PVP assumed for the diffusion process cannot explain the fact that the minimum differential capacity observed for PVP differs little from that given by the common organic compound of a non-polymer or from that observed for *N*-vinyl-2-pyrrolidone,<sup>14)</sup> which is a component monomer of PVP. Therefore, it may be assumed that the adsorbed PVP at the interface takes a configuration of a spread or flatten form of the chain instead of the spherical form. Moreover, consistent with the above conclusion, the adsorbed number of constitutive segments per unit of area is nearly constant, independent of the  $\bar{M}$ , as has been mentioned previously.

The authors would like to express their acknowledgements to Dr. Shigemitsu Nomoto for his valuable discussions. The financial aid from the Ministry of Education for this work is gratefully acknowledged.

14)  $D = D_0(1 + \alpha)^T$  for  $\alpha$  and  $D = D_0 \exp(-Q/RT)$  for  $Q$ , where  $D_0$  and  $Q$  can be obtained by experimental determinations of the diffusion coefficient at two or more temperatures.

14) This Bulletin, to be published.